Supplementary material: Trapping flocking particles with asymmetric obstacles

Raul Martinez, Francisco Alarcon,
Juan Luis Aragones, and Chantal Valeriani

February 12, 2020

A On the probability of passing the wall from both sides

In the main text we have argued the trapping of the Vicsek particles on the convex side of the funneled wall because, as long as the flock is aligned with the wall, the probability of going into the convex side of the wall in much higher than the probability of passing in the opposite direction. In this section, we show an example to justify this assumption. We choose a system with $N = 2000$, $L = 32$, $\eta = 0.1$, $\delta = 0.6$, $d_c = 2$ and $\alpha = 30$ degrees, in which a complete trapping of metric Vicsek particles occurs. In addition, we set the initial positions of the particles to be aligned and parallel to the funneled wall, in one case on the concave side of the wall (Fig. 1A) and in the other on the concave side (Fig. 1B). Then, we compute the number of particles that enter into the channel during the first 600 iterations, obtaining a passing rate of $N_{in} = 1.972$ particles per iteration. On the contrary, the rate of particles leaving the channel in the steady state, between iterations 5000 to 10000, is of about $N_{out} = 0.002$ particles per iteration. As it can be seen in Fig. 1C, we are counting the number of particles entering into the channel, N_{in}, during a transitory state, while the number of particles escaping the channel, N_{out}, is obtained once the steady state has been reached. Thus, we can estimate the relationship between the probability of passing towards the concave side of the wall, $P_{concave}$, and the probability of passing towards the convex side P_{convex} as:

$$\frac{P_{concave}}{P_{convex}} = 0.5\frac{N_{in}}{N_{out}} \approx 0.0005 \tag{1}$$

where the factor 0.5 takes into account that in the steady state particles can escape the channel through both walls. Therefore, as long as the flock is aligned with the wall and η small enough, the difference in probabilities of passing from the concave to the convex side explains the trapping inside the channel.

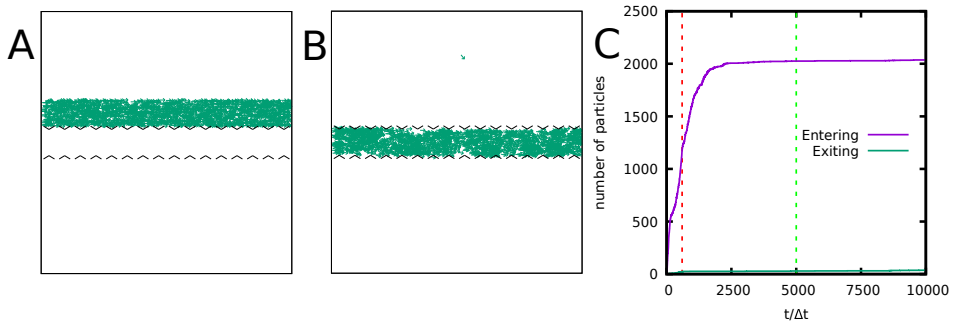

Fig. S 1: A) Snapshot of the initial condition. B) Snapshot of the steady state. C) Time evolution of the number of particles escaping (green line) and entering (violet line) into the channel. The horizontal red dashed line indicates the time interval where N_{in} is evaluated and the light green dashed line points the time interval where N_{out} has been computed.

We have applied the same method to determine the probability of particles escaping and entering the channel as a function of the opening of the funnels δ. We set the initial positions of the particles to be aligned and parallel to the funneled wall, in one case on the concave side of the wall (Fig. 1A) and in the other on the concave side (Fig. 1B). To compute the entering flux we only used the initial time steps, until a total of $N/4$ particles entered the channel, and averaged aver 10 different trajectories, while the leaving flux is computed along one simulation of 50000 steps. Because of these selected initial configurations we can estimate the relationship between the probability of passing towards the concave side of the wall, $P_{concave}$, and the probability of passing towards the convex side P_{convex} from these fluxes. As it can be seen in figure 2, the both probabilities, entering and leaving the channel, increase with δ, but the leaving probability increases at a much more higher rate. The probability ratio $\frac{P_{concave}}{P_{convex}}$ increases with δ exponentially and will eventually reach a value of one. Therefore, the trapping of Vicsek particles is less effective as δ increases.

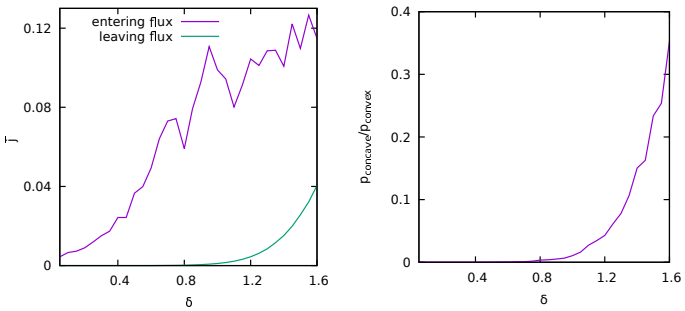

Fig. S 2: Left, normalized entering and leaving flux ($\bar{j}$, as defined in the main text and used in figure 4) as a function of δ. Right, The ratio between the probabilities of entering and leaving the channel as a function of δ. The values $\eta = 0.1$, $\alpha = 30$ degrees, $d_c = 2$, $L = 32$ and $N = 2000$ remain fixed in both graphics.

B Dependence on the bouncing rules

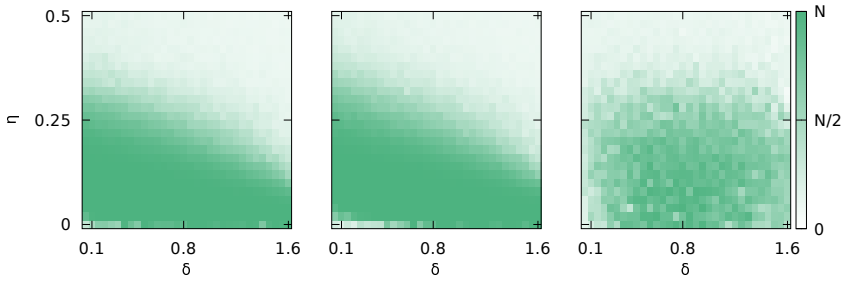

Fig. S 3: Number of particles trapped in the steady state (after 50000 iterations) as a function of the opening length of the funnels, δ, and Vicsek noise, η, in the case of an aligning bouncing rule (left), an elastic bouncing rule (center) and a repulsive bouncing rule (right). Vicsek particles with swimming speeds of $v = 0.2$ in between two parallel walls of funnels with $\alpha = 30$ degrees and $d_c = 2$.

C Dependence on the swimming speed

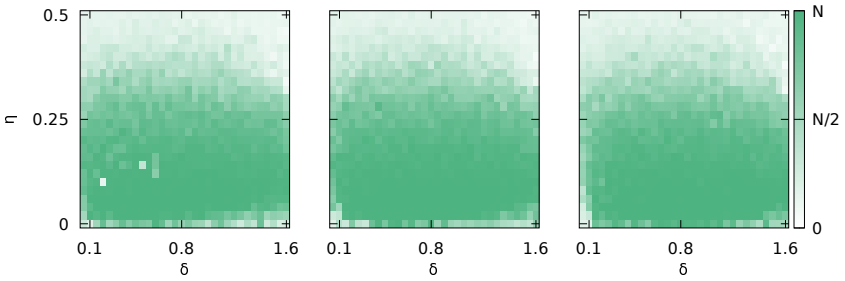

Fig. S 4: Number of particles trapped in the steady state (after 200000 iterations) as a function of the opening length of the funnels, δ, and Vicsek noise, η, in the case of an aligning bouncing rule (left), an elastic bouncing rule (center) and a repulsive bouncing rule (right). Vicsek particles with swimming speeds of $v = 0.004$ in between two parallel walls of funnels with $\alpha = 30$ degrees and $d_c = 2$.

D Comparison with Drocco *et al*

Our results significantly differ from those reported in Ref. [1] and thus, we have carried out a thorough comparison. In Ref. [1], the authors consider excluded-volume Vicsek particles that depending on the particles' size rectifies towards one side or the other of the funneled wall. Since our particles are punctual, this comparison is restricted to the low size limit of their particles. There are three relevant differences between our work and theirs. The Vicsek velocity v: they use $v = 0.004$ while se use $v = 0.2$; the bouncing rule: we use aligning while they use repulsive; and the boundaries: we use periodic boundary conditions while they use repulsive ones.

We have qualitatively reproduced the geometry reported in Ref. [1]; a single funneled wall in a square simulation box of side length $L = 30$ bounded by repulsive wall. First, as shown in section C, the bouncing rule is not important for the behaviour of the system at such low velocities. To investigate the role of the two other differences, we launched two funnel geometries, one with $\alpha = 60$ degrees, the angle used in Ref. [1] and another with $\alpha = 30$ degrees, being $d_c = 1$ and $\delta = 0.4$. For each of these geometries, we simulated a system with repulsive boundaries and another with periodic boundary conditions along in the axis parallel to the wall, while keeping repulsive boundaries

in the other axis. We defined the parameter $r = N_{top}/N$, where N_{top} is the number of particles in the top chamber averaged over the last half of the run, which has a total of 100000 iterations. When using $\alpha = 60$ degrees with repulsive boundaries (figure 5, left panel), we obtained $r = 0.959$, in good agreement with the results in Ref. [1], while applying periodic boundary conditions in one direction, we obtained $r = 0.931$. Repeating the same simulations with $\alpha = 30$ degrees, we obtained $r = 0.053$ for the repulsive boundary case and $r = 0.015$ applying periodic boundary conditions (figure 5, right panel). Therefore, we conclude that changing the geometry of the funnel wall seems to be enough to achieve trapping at the other side of the chamber. In addition, the periodic boundary conditions enhances the described collective trapping described in our paper. This is because both factors increase the tendency of the flocks to align with the wall of funnels, which is crucial for the collective trapping behavior to occur.

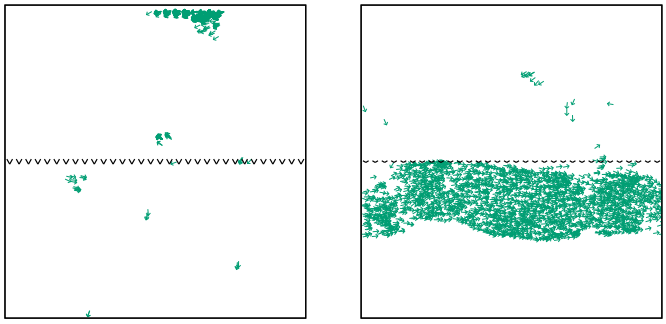

Fig. S 5: Left, a reproduction of the geometry used in the paper by Drocco and others[1]. Right, we recover our geometry by changing the angle of the chevrons and using periodic boundary conditions in one direction.

E A Vicsek-like nematic alignment model: trapping also occurs

In physical systems, steric interactions between the different rod-shaped elements can induce nematic alignment, making the study of systems that show this type of collective behavior very interesting from both the theoretical and experimental point of view. In this section, we use the same system as in the rest of the manuscript, except that we use a modification in the inter particle interaction rules to produce nematic alignment [4].

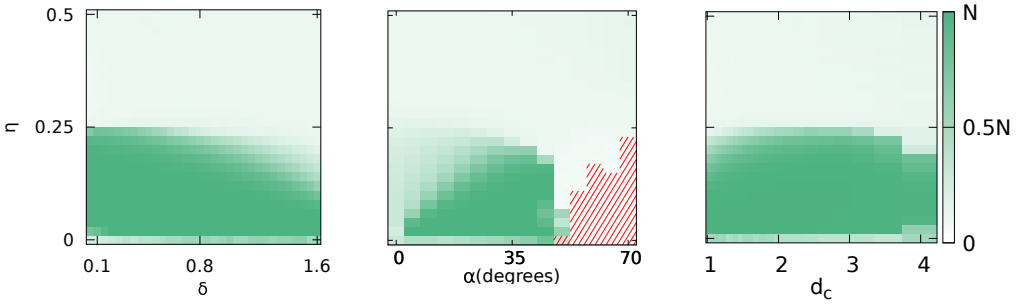

Fig. S 6: Trapping of particles that follow the equivalent of a metrico Vicsek model but interactin via the nematic alignment rule presented in eq 3. Left, trapping as dependent on η and γ, with $d_c = 2$ and $\alpha = 30$ degrees. Center, dependence on η and α, with $\delta = 1$ and $d - c = 2$, in the red dashed region particles get trapped in the concave side of each individual chevron. Right, dependence on η and d_c, with $\delta = 0.5$ and $\alpha = 30$ degrees.

The Vicsek alignment rule, as exposed in equation 2 of the main text, reads:

$$\theta_i(t + \Delta t) = \arg\left[\sum_{j \in \mathcal{N}_i(t)} e^{i\theta_j(t)}\right] + 2\pi\eta\zeta \tag{2}$$

Where θ_j are the orientations of the neighbors of particle i. In this section we use, instead:

$$\theta_i(t + \Delta t) = \arg\left[\sum_{j \in \mathcal{N}_i(t)} \text{sign}[\cos(\theta_k - \theta_j)] e^{i\theta_j(t)}\right] + 2\pi\eta\zeta \tag{3}$$

Under this interaction rule, the steady state of the system at low η exhibis nematic order.

The same configuration of obstacles that we used with the Vicsek model is also capable of trapping particles in this other system. In figure 6 we can see the equivalent of first column of figure 2 from the main text, and there is an evident similarity. Thus, we can conclude that the results presented in this paper are also of interest for the study of systems showing nematic order.

References

[1] Drocco, J. A., Reichhardt, C. O., & Reichhardt, C. (2012). Bidirectional sorting of flocking particles in the presence of asymmetric barriers. *Physical Review E, 85(5), 056102.*

[2] Galajda, P., Keymer, J., Chaikin, P., & Austin, R. (2007). A wall of funnels concentrates swimming bacteria. *Journal of bacteriology, 189(23), 8704-8707.*

[3] Wan, M. B., Reichhardt, C. O., Nussinov, Z., & Reichhardt, C. (2008). Rectification of swimming bacteria and self-driven particle systems by arrays of asymmetric barriers. *Physical review letters, 101(1), 018102.*

[4] Ginelli, F., Peruani, F., Bär, M., & Chaté, H. (2010). Large-scale collective properties of self-propelled rods. *Physical review letters, 104(18), 184502.*